LANGMUIR

Article

pubs.acs.org/Langmuir

Influence of Divalent Cations on Deformation and Rupture of Adsorbed Lipid Vesicles

Marija Dacic,[†,‡,#] Joshua A. Jackman,[†,‡,#] Saziye Yorulmaz,[†,‡] Vladimir P. Zhdanov,[†,‡,∥] Bengt Kasemo,[⊥] and Nam-Joon Cho*[,†,‡,§]

[†]School of Materials Science and Engineering, Nanyang Technological University, 50 Nanyang Avenue 639798, Singapore

[‡]Centre for Biomimetic Sensor Science, Nanyang Technological University, 50 Nanyang Drive 637553, Singapore

[§]School of Chemical and Biomedical Engineering, Nanyang Technological University, 62 Nanyang Drive 637459, Singapore

[∥]Boreskov Institute of Catalysis, Russian Academy of Sciences, Novosibirsk 630090, Russia

[⊥]Department of Physics, Chalmers University of Technology, 41296 Göteborg, Sweden

Supporting Information

ABSTRACT: The fate of adsorbed lipid vesicles on solid supports depends on numerous experimental parameters and typically results in the formation of a supported lipid bilayer (SLB) or an adsorbed vesicle layer. One of the poorly understood questions relates to how divalent cations appear to promote SLB formation in some cases. The complexity arises from the multiple ways in which divalent cations affect vesicle−substrate and vesicle−vesicle interactions as well as vesicle properties. These interactions are reflected, e.g., in the degree of deformation of adsorbed vesicles (if they do not rupture). It is, however, experimentally challenging to measure the extent of vesicle deformation in real-time. Herein, we investigated the effect of divalent cations (Mg^{2+}, Ca^{2+}, Sr^{2+}) on the adsorption of zwitterionic 1,2-dioleoyl-*sn*-glycero-3-phosphocholine (DOPC) lipid vesicles onto silicon oxide- and titanium oxide-coated substrates. The vesicle adsorption process was tracked using the quartz crystal microbalance-dissipation (QCM-D) and localized surface plasmon resonance (LSPR) measurement techniques. On silicon oxide, vesicle adsorption led to SLB formation in all cases, while vesicles adsorbed but did not rupture on titanium oxide. It was identified that divalent cations promote increased deformation of adsorbed vesicles on both substrates and enhanced rupture on silicon oxide in the order $Ca^{2+} > Mg^{2+} > Sr^{2+}$. The influence of divalent cations on different factors in these systems is discussed, clarifying experimental observations on both substrates. Taken together, the findings in this work offer insight into how divalent cations modulate the interfacial science of supported membrane systems.

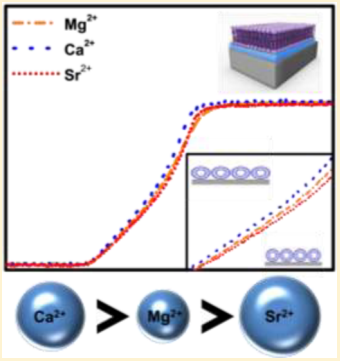

INTRODUCTION

Lipid membranes are an important component of biological systems, and have diverse roles involving compartmentalization, transport, and signaling.[1,2] Due to the complexity of biological membranes, there is significant interest in developing simplified models based on phospholipid bilayers in order to study molecular self-assembly and biophysical processes related to membrane functions such as cell adhesion and ligand−receptor interactions.[3−5] In particular, solid-supported lipid bilayers (SLBs) are an attractive model membrane experimental platform because the support offers improved physical stability and also enables the use of highly surface-sensitive analytical tools.[6−8]

The most common method to fabricate SLBs includes adsorption of lipid vesicles accompanied by their fusion and rupture occurring via one of numerous possible channels.[6] Typically, in cases of bilayer formation, single, adsorbed vesicles either rupture upon interaction with the solid support, or vesicles adsorb and remain intact until reaching a critical surface coverage, which initiates the rupture process.[3] Experimentally, it has been widely observed that silica-based materials[9,10] are excellent substrates to promote SLB formation from conventional zwitterionic lipid vesicles, while such vesicles typically adsorb but do not rupture on many other substrates such as gold[9] and titanium oxide.[10] Given the empirical nature of these findings, there have been extensive experimental efforts to understand how vesicle properties (lipid composition,[11,12] lamellarity,[13] size,[10] osmotic pressure[10]), environmental conditions (solution pH,[14] temperature,[10,15] ionic strength[16]), and substrate properties (atomic composition,[10] crystallinity,[17] roughness[18]) affect SLB formation.

To facilitate the corresponding studies, numerous label-free measurement techniques such as quartz crystal microbalance-dissipation (QCM-D),[19] surface plasmon resonance (SPR),[20] atomic force microscopy,[21] interferometric scattering,[22] and localized surface plasmon resonance (LSPR)[23] have been employed in order to track the kinetic stages of vesicle adsorption and rupture. Arising from the combination of

Received: February 7, 2016
Revised: April 30, 2016
Published: May 16, 2016

DOI: 10.1021/acs.langmuir.6b00439
Langmuir 2016, 32, 6486−6495

systematic investigations and increasingly sophisticated measurement techniques, there is a growing appreciation that the observed dependence of SLB formation on the solid support is strongly related to the vesicle−substrate interaction, especially the degree of deformation of adsorbed vesicles prior to vesicle rupture.[10,24,25] If there is a strong vesicle−substrate interaction, then an adsorbed vesicle will undergo greater deformation, which increases the membrane stress near the rim of the vesicle−substrate contact area where the membrane bending is appreciable.[26−28] Experimentally, however, direct measurement of vesicle deformation at low surface coverages has proven difficult for small vesicles (<200 nm diameter) and the current model is largely inferred from physical models that relate the vesicle−substrate contact energy to the extent of vesicle deformation as validated by theoretical calculations and simulations.[28−33] Atomic force microscopy experiments have investigated the deformation of individual, adsorbed phosphatidylcholine vesicles on glass at low surface concentrations.[21,34] Recently, it was reported that highly surface-sensitive LSPR measurements can be used to quantify deformation of adsorbed vesicles in different membrane phase states and to distinguish the extent of vesicle deformation on silicon oxide and titanium oxide.[15,25,35] Such tools open the door to unraveling how complex environmental factors influence the SLB formation process by providing measurement capabilities to track vesicle adsorption and deformation on solid supports.

In this regard, one of the most fundamental issues concerns understanding how ions present in solution affect vesicle adsorption and SLB formation. Several studies so far have been able to change the conventional scenarios of vesicle adsorption by introducing different types of ions.[11,12,36,37] For example, under certain conditions, calcium ions are reported to promote SLB formation of mixed phosphatidylcholine−phosphatidylserine lipid vesicles on titanium oxide due to an ion bridging effect between the titanium oxide surface and phosphatidylserine lipid.[12] Concerning zwitterionic phosphatidylcholine lipid vesicles, a comprehensive study by Seantier and Kasemo explored the effect of different monovalent and divalent cations on 1-palmitoyl-2-oleoyl-*sn*-glycero-3-phosphocholine (POPC; one saturated and one unsaturated tail) SLB formation on silicon oxide.[38] Divalent ions were, based on trends in the QCM-D data, concluded to have a much stronger enhancing effect on bilayer formation, reflected in a lower critical coverage for the vesicle-to-bilayer transformation. Among the divalent ions, the enhancing order was $Mg^{2+} > Ca^{2+} > Sr^{2+}$. The fact that different divalent ions have different quantitative effects at the same ionic strength shows that details of the ions like size, polarizibility, and hydration shell thickness play a role. The suggested and qualitative mechanistic explanation was then that the different divalent cations affect the vesicle−substrate interaction and vesicle stability to varying extents, which leads to different degrees of deformation of adsorbed vesicles for the respective ion types.

Additional literature reports[36,39−45] also indicate that certain types of divalent cations (typically Ca^{2+}) induce stronger vesicle-surface interaction, however, the relative effects of different divalent cations on SLB formation remain untested in direct comparison for other lipid compositions besides POPC lipid, especially in the context of comparing the extent of vesicle deformation on the substrate. Considering that divalent cations have different effects on the membrane properties of fluid-phase, zwitterionic lipid bilayers comprising phospholipids with one or two unsaturated tails, expanding the scope of investigated lipids to a lipid with two unsaturated tails would complement existing knowledge about POPC SLB systems, and shed insight into whether the observed trend ($Mg^{2+} > Ca^{2+} > Sr^{2+}$) of accelerating SLB formation is a general phenomenon. Indeed, in lipid bilayers, PC lipids with one or two unsaturated chains have different free rotation energies and hence the interaction between PC lipid headgroups and divalent cations varies due to the balance that must be achieved between the ion-dipole interaction and the free rotational entropy of the headgroup.[46]

Moreover, surface-sensitive measurements probing the relative deformation of adsorbed vesicles on silicon oxide at surface concentrations below the critical coverage as well as on other substrates such as titanium oxide where vesicle adsorption and deformation occur without rupture would significantly aid our understanding of the relationship between accelerating SLB formation and the nature of the vesicle−substrate interaction. Importantly, the aforementioned LSPR measurements can be performed in real-time and measure the relevant extent of ion-induced vesicle deformation in different solution conditions that occurs during the dynamic process leading to vesicle rupture and SLB formation. Indeed, such information can clarify the relative degree of membrane tension in the adsorbed vesicles, offering insight into the fusogenic character of adsorbed vesicles relative to various ionic conditions.

The goal of this study is to investigate how divalent cations affect the adsorption behavior of zwitterionic 1,2-dioleoyl-*sn*-glycero-3-phosphocholine (DOPC) lipid vesicles on two different solid supports, namely silicon oxide and titanium oxide. Silicon oxide was chosen because it is a common substrate for vesicle adsorption and rupture leading to SLB formation, while titanium oxide was selected because zwitterionic lipid vesicles typically adsorb but do not rupture on the substrate. DOPC is a popular lipid to fabricate SLBs and has two unsaturated tails. Hence, our findings provide a useful comparison with the POPC lipid system in order to understand how different divalent cations affect SLB formation arising from lipids with one or two unsaturated tails. Furthermore, the choice of titanium oxide as an additional substrate allows us to determine whether similar effects of ion-induced vesicle deformation occur on other solid supports. Systematic experiments were conducted in 10 mM Tris buffer [pH 7.5] with 150 mM NaCl without or with 5 mM $MgCl_2$, $CaCl_2$ or $SrCl_2$ added. QCM-D measurements were performed in order to monitor the acoustic mass and viscoelastic properties of adsorbed vesicle layers in intermediate and saturated coverage regimes. LSPR measurements were also performed on silicon oxide- and titanium oxide-coated gold nanodisk arrays (which are the LSPR sensing components) in order to evaluate the vesicle adsorption kinetics based on changes in the local refractive index due to vesicle adsorption and deformation, paying particular attention to the rate of change in the LSPR signal which, at a given deposition rate of vesicles on the surface, is proportional to the extent of vesicle deformation in the low coverage regime.[15,25,35] Importantly, the two measurement techniques rely on different physical principles with different corresponding surface sensitivities, and provide complementary information about the deformation of adsorbed vesicles in different surface coverage regimes (Figure 1). The QCM-D technique is sensitive to the adsorbed lipid mass and hydrodynamically coupled solvent mass such that, conceptually, a less deformed vesicle would register greater measurement responses because there is a larger amount of coupled solvent.

DOI: 10.1021/acs.langmuir.6b00439
Langmuir 2016, 32, 6486−6495

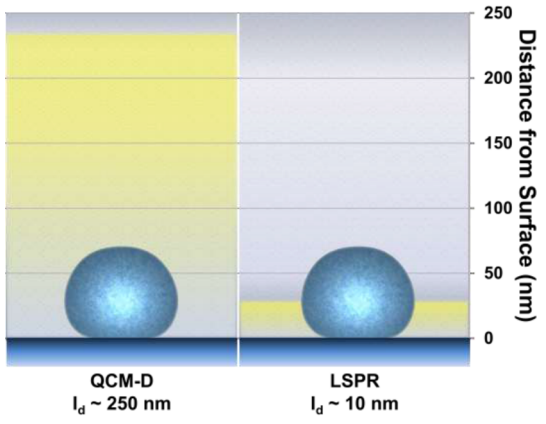

Figure 1. Comparison of the surface sensitivity of QCM-D and LSPR measurements for probing vesicle adsorption. QCM-D measurements have a penetration length of around 250 nm, while LSPR measurements are more highly surface sensitive, with the decay length of the evanescent field around 10 nm. As such, the LSPR measurement capabilities are particularly useful for probing the deformation of adsorbed vesicles.

By contrast, the LSPR technique is sensitive to the adsorbed lipid mass only because it has a different refractive index than the surrounding medium, and a more deformed vesicle is known to register a greater measurement response because the lipid mass is, on average, closer to the sensor surface. These measurement capabilities enable the first direct experimental evidence of divalent cation-induced contribution to vesicle deformation and allow us to quantitatively compare the relative deformation of adsorbed vesicles in the presence of different divalent cations. Taken together, the experimental findings scrutinize the extent of vesicle deformation on the two test substrates and clarify the ways in which divalent cations influence vesicle adsorption and rupture.

MATERIALS AND METHODS

Buffer Preparation. Tris (hydroxymethyl)aminomethane (Tris) was obtained from Amresco (Solon, OH) and sodium chloride, magnesium chloride, calcium chloride, and strontium chloride salts as well as sodium dodecyl sulfonate were obtained from Sigma-Aldrich (St. Louis, MO). The reference buffer solution contained 10 mM Tris and 150 mM NaCl, and 5 mM $MgCl_2$, $CaCl_2$ or $SrCl_2$ was added depending on the sample. After all the salts were added, the buffer solution was titrated to pH 7.5 using hydrochloric acid. All solutions were prepared with 18.2 MΩ·cm Milli-Q-treated deionized water (Millipore, Billerica, MA).

Vesicle Preparation. Zwitterionic 1,2-dioleoyl-*sn*-glycero-3-phosphocholine (DOPC) lipid was obtained from Avanti Polar Lipids (Alabaster, AL). Small unilamellar vesicles composed of DOPC lipid were prepared by the extrusion method.[47] As-supplied lipids in the powder state were dissolved in chloroform and treated with nitrogen air to form a dried lipid film, which was subsequently stored in a vacuum desiccator for at least 24 h. The dried lipid film was then dissolved in the reference buffer (10 mM Tris [pH 7.5] and 150 mM NaCl) at a stock concentration of 5 mg/mL and vortexed for 2 min. Extrusion was next performed through 50 nm diameter track-etched polycarbonate membranes a minimum of 17 times and the obtained vesicle solutions were stored at 4 °C until experiment. Immediately before experiment, the stock lipid solutions were diluted in the relevant buffer to a concentration of 0.1 mg/mL for the QCM-D experiments and 0.05 mg/mL for the LSPR experiments. For each measurement technique, all experiments were conducted with a single vesicle preparation in order to avoid differences in vesicle number concentration and size distribution.

Dynamic Light Scattering (DLS). In order to determine the vesicle size distribution, DLS measurements were performed on freshly extruded vesicles. A 90Plus particle size analyzer (Brookhaven Instruments, Holtsville, NY) with a 658.0 nm monochromatic laser was used. The scattering angle at which the measurements were taken was 90°. The intensity-weighted size distribution of vesicles was generated from the measured intensity autocorrelation function, and the cumulant method was employed in order to obtain the intensity-weighted Gaussian profile of the vesicle size distribution, which included the average effective vesicle diameter and polydispersity. The average diameter of vesicle samples was around 75 nm.

Quartz Crystal Microbalance-Dissipation (QCM-D). The kinetics of vesicle adsorption onto the solid supports were monitored by using a Q-Sense E4 instrument (Biolin Scientific, Göteborg, Sweden). The changes in resonance frequency and energy dissipation of an oscillating silicon oxide- or titanium oxide-coated 5 MHz AT-cut quartz crystal sensor chip (Biolin Scientific) were simultaneously recorded as a function of time. Prior to each experiment, the sensor chips were sequentially rinsed with deionized water and ethanol, followed by drying with a stream of nitrogen air. The sensor chips were then subjected to oxygen plasma treatment (Harrick Plasma, Ithaca, NY) for 1 min at maximum radiofrequency power. All QCM-D measurements were conducted under continuous flow conditions, with the flow rate set at 41.8 μL/min and controlled by a Reglo Digital peristaltic pump (Ismatec, Glattbrugg, Switzerland). The temperature of the flow cell was fixed at 25.00 ± 0.5 °C. The measurement data were collected at multiple odd overtones and the reported data was obtained at the fifth (n = 5) overtone. Measurement data are expressed as the mean ± standard deviation of the mean where appropriate (n = 4 measurements). Statistical analysis was performed with the OriginPro 9 software program (OriginLab Corporation, Northampton, MA, USA). Differences between all the results were analyzed using one-way analysis of variance (ANOVA), followed by a posthoc Bonferroni test. $p < 0.05$ was considered to be statistically significant (*).

Localized Surface Plasmon Resonance (LSPR). Ensemble-averaged LSPR measurements based on the indirect nanoplasmonic sensing principle were performed in optical transmission mode by using an Insplorion XNano instrument (Insplorion AB, Göteborg, Sweden), as previously described.[35] The sensor chips (Insplorion AB) consisted of well-separated ca. 120 nm diameter gold nanodisks, which were fabricated on a glass substrate by hole-mask colloidal lithography. The gold nanodisks were covered by a thin, sputter-coated layer of titanium oxide or silicon oxide for the vesicle adsorption experiments. Prior to each experiment, the sensor chips were sequentially rinsed with deionized water and ethanol, followed by drying with a stream of nitrogen air. The sensor chips were then subjected to oxygen plasma treatment (Harrick Plasma, Ithaca, NY) for 1 min at maximum radiofrequency power. All LSPR measurements were conducted at ambient room temperature under continuous flow conditions, with the flow rate set at 70 μL/min and controlled by a Reglo Digital peristaltic pump (Ismatec, Glattbrugg, Switzerland).

RESULTS

QCM-D Measurements. In order to track vesicle adsorption on the silicon oxide and titanium oxide substrates, QCM-D experiments were conducted. Changes in resonance frequency (Δf) and energy dissipation (ΔD) were monitored as a function of time, and are related to the mass and viscoelastic properties of the adsorbate, respectively.[9] If a vesicle adsorbs onto the substrate, then there will typically be a negative Δf shift and a positive ΔD shift. In all experiments, a baseline signal was first recorded in the appropriate buffer solution followed by the addition of 0.1 mg/mL lipid vesicles in an identical buffer solution at t = 5 min. The results obtained on the silicon oxide and titanium oxide substrates are reported below.

DOI: 10.1021/acs.langmuir.6b00439
Langmuir 2016, 32, 6486−6495

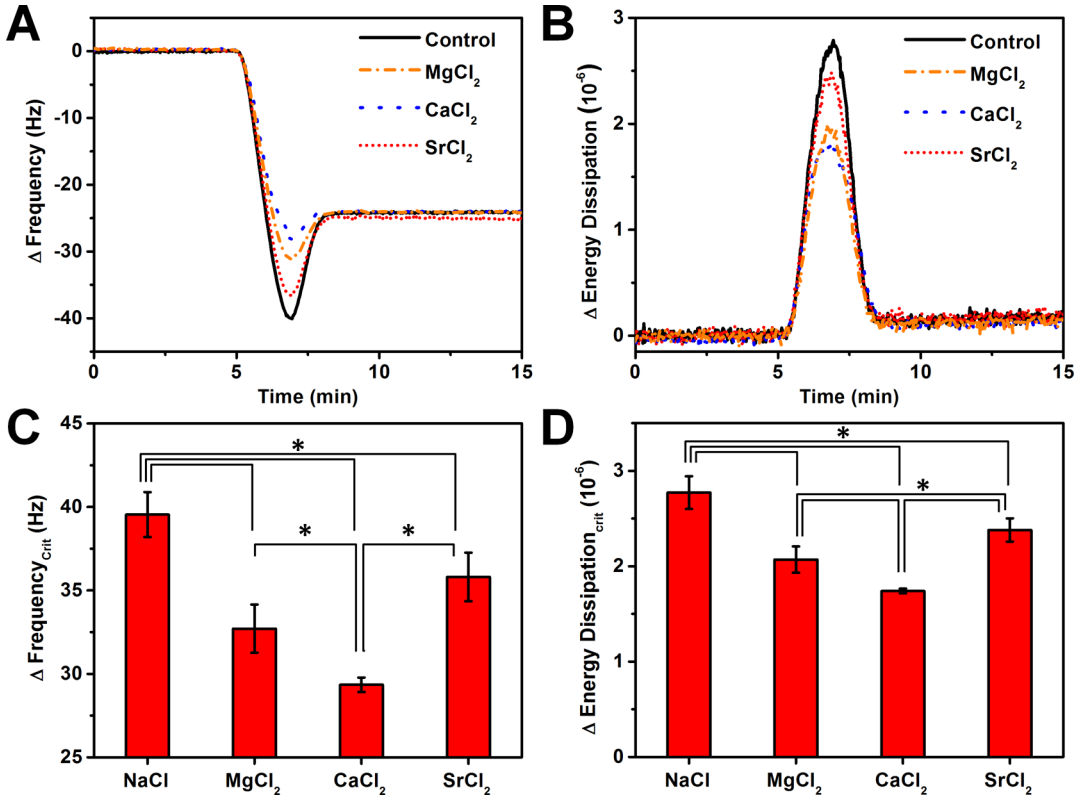

Figure 2. Effect of divalent cations on vesicle adsorption and rupture on silicon oxide. QCM-D measurements were performed and vesicles were added at t = 5 min. (A) Δf shift and (B) ΔD shift as a function of time. Mean and standard deviation of the (C) $|\Delta f_c|$ and (D) ΔD_c values obtained in quadruplicate measurements. The control experiment contained the same vesicle preparation and buffer conditions without divalent cations.

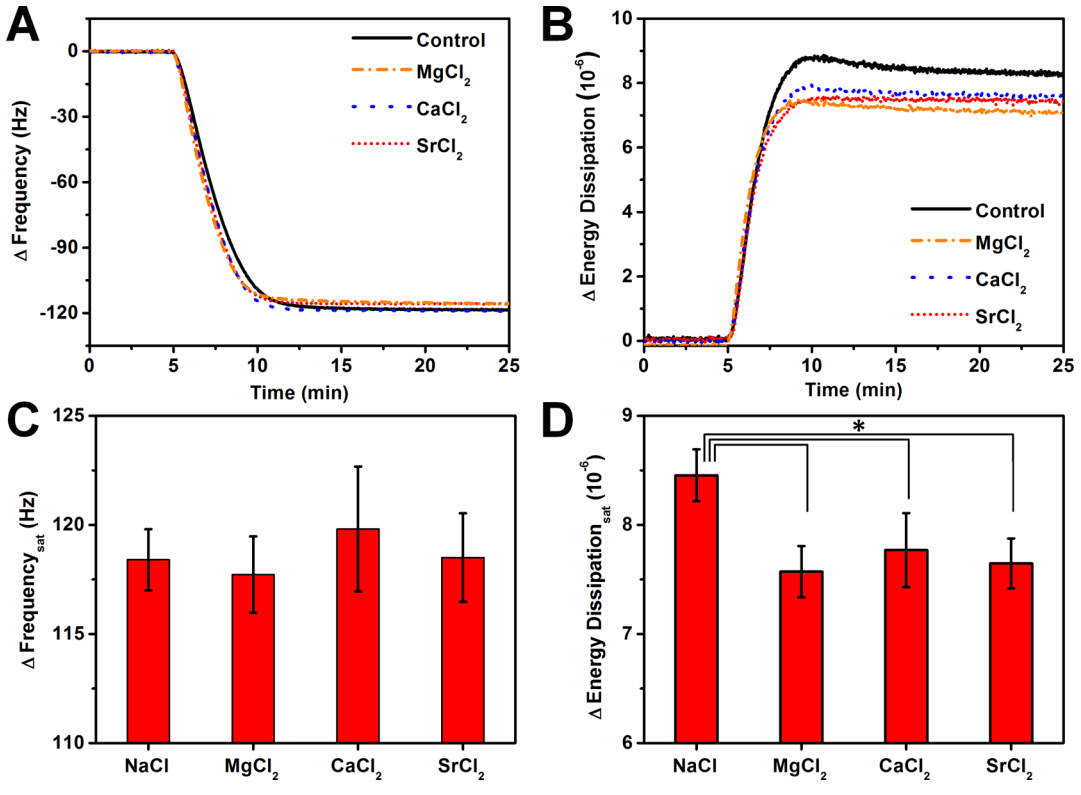

Figure 3. Effect of divalent cations on vesicle adsorption onto titanium oxide. QCM-D measurements were performed and vesicles were added at t = 5 min. (A) Δf shift and (B) ΔD shift as a function of time. Mean and standard deviation of (C) $|\Delta f_c|$ and (D) ΔD_c values obtained in quadruplicate measurements. The control experiment contained the same vesicle preparation and buffer conditions without divalent cations.

DOI: 10.1021/acs.langmuir.6b00439
Langmuir 2016, 32, 6486−6495

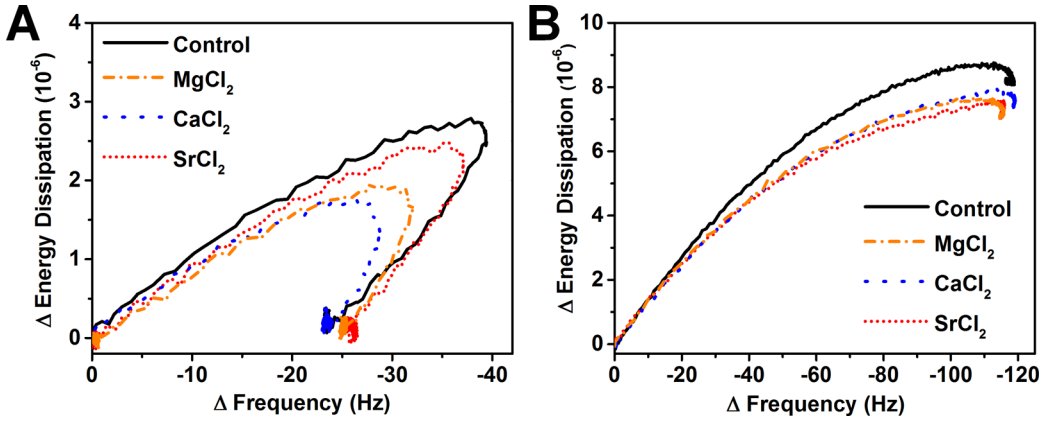

Figure 4. Analysis of vesicle adsorption by $\Delta D/\Delta f$ plots. The vesicle adsorption processes on (A) silicon oxide and (B) titanium oxide are represented as a function of the energy dissipation shift versus the frequency shift. The control experiment contained the same vesicle preparation and buffer conditions without divalent cations.

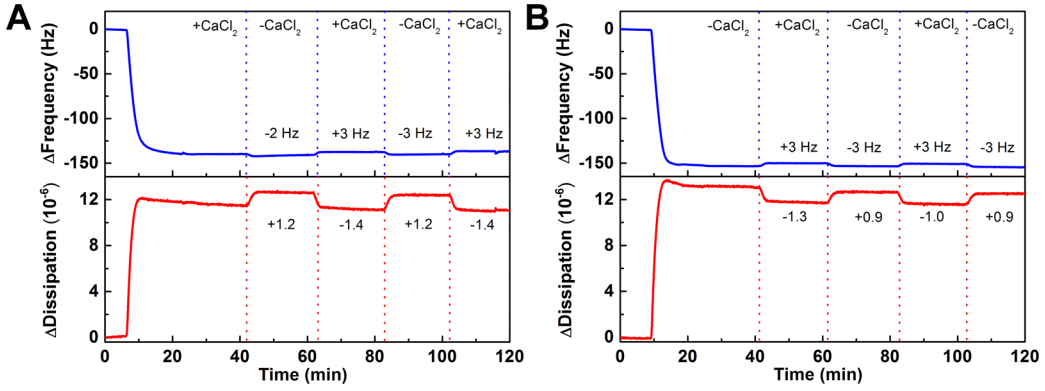

Figure 5. Reversible control of vesicle deformation by addition and removal of divalent cations. QCM-D measurements were performed, and DOPC lipid vesicles were added onto a titanium oxide substrate at approximately t = 10 min. (A) Vesicles were suspended in 10 mM Tris buffer [pH 7.5] with 150 mM NaCl and 5 mM $CaCl_2$ and, after vesicle adsorption reached saturation, the solution buffer was exchanged back and forth approximately every 20 min with the equivalent buffer that had no $CaCl_2$. (B) The opposite experiment was also performed whereby the vesicles were initially suspended in 10 mM Tris buffer [pH 7.5] with 150 mM NaCl and no $CaCl_2$, and then the solution buffer was exchanged back and forth approximately every 20 min with the equivalent buffer that had 5 mM $CaCl_2$.

Silicon Oxide. On silicon oxide, the initial adsorption of lipid vesicles onto the substrate proceeded until reaching a critical surface coverage of adsorbed vesicles (Figure 2A,B). The critical coverage is denoted by inflection points in the measurement signals corresponding to Δf_c, ΔD_c, Δt_c. After reaching the critical coverage, vesicle rupture became the predominant process, and the release of hydrodynamically coupled solvent mass resulted in a positive Δf shift and a negative ΔD shift.

Compared to the measurement baseline values, the final Δf and ΔD shifts were approximately −26 Hz and $<0.3 \times 10^{-6}$, respectively, which indicate SLB formation.[9] While SLB formation was observed in all cases, there were quantitative differences in the corresponding kinetics that could be tracked based on the measurement values at the critical coverage.

A comparison of the Δf_c and ΔD_c values, obtained for vesicle adsorption in the presence of different divalent cations, is shown in Figure 2C,D. The average Δf_c and ΔD_c values for the reference case without divalent cations were −38 Hz and 2.8×10^{-6}, respectively. By contrast, the corresponding values for the Ca^{2+} case were −28 Hz and 1.8×10^{-6}, respectively. The values for the Mg^{2+} and Sr^{2+} cases were between those of the two aforementioned cases. At the same time, no statistically significant dependence of Δt_c on the type of divalent ion was observed, suggesting that the smaller Δf_c and ΔD_c values reflect a difference in the extent of deformation of adsorbed vesicles rather than the absolute surface density of adsorbed vesicles (Figure S1). Hence, divalent cations appear to strengthen the lipid−substrate interaction in order to promote SLB formation in the following order: $Ca^{2+} > Mg^{2+} > Sr^{2+}$.

Titanium Oxide. Monotonous kinetics observed in similar experiments on titanium oxide (Figures 3A,B) are indicative of vesicle adsorption until forming a close-packed, saturated adlayer. No vesicle rupture resulting in SLB formation was observed in this case for any ion type. Under all tested conditions, the final Δf shifts were around −118 Hz (Figure 3C). However, there was a quantitative difference in the ΔD shifts between the reference case and the divalent ion cases (Figure 3D). The final ΔD shift for the reference case was around 8.5×10^{-6}, while the ΔD shifts were around 7.5×10^{-6} for the divalent ion cases. This finding supports that divalent ions increase the rigidity of the whole, adsorbed vesicle layer, which could be due to increased deformation and/or increased rigidity of individual vesicles.

Comparison of Vesicle Adsorption on Silicon Oxide and Titanium Oxide. To further analyze the QCM-D measurement data, $\Delta D/\Delta f$ plots were constructed in order to understand how the adsorbate properties change independently of time[48]

DOI: 10.1021/acs.langmuir.6b00439
Langmuir 2016, 32, 6486−6495

(Figure 4). On silicon oxide, vesicle adsorption and rupture were indicated by two stages in the adsorption process, with the cusp between the two stages indicating the vesicle-to-bilayer structural transformation[48] (Figure 4A). The first stage consists of vesicle adsorption and fusion, while the second stage involves vesicle rupture leading to SLB formation. Interestingly, the slope of the initial stage of vesicle adsorption for Δf shifts less than −15 Hz was quite similar for all divalent cation cases. However, the position of the cusp in the Δf, ΔD coordinate system exhibited a strong dependence on the type of divalent cation, with Ca^{2+} ions inducing onset of the structural transformation at the smallest Δf, ΔD values. Hence, subtle changes in the particular, divalent cations increase the deformation of adsorbed vesicles on silicon oxide in line with the aforementioned kinetic analysis. On the other hand, vesicle adsorption on titanium oxide exhibited only one stage, which is consistent with monotonic adsorption (Figure 4B). The $\Delta D/\Delta f$ slope was appreciably greater (by about 30%) than the corresponding one for vesicle adsorption on silicon oxide, indicating that each vesicle has a greater contribution to the energy dissipation in the titanium oxide case. In other words, the deformation of adsorbed vesicles on titanium oxide is less than that of the same vesicles on silicon oxide, which has also been shown by LSPR measurements for vesicles in monovalent salt conditions.[25] Furthermore, all tested types of divalent cation appear to have similar effects on the adsorption behavior of vesicles on titanium oxide and induced greater vesicle deformation in comparison to the control experiment without divalent cations.

Reversible Deformation of Adsorbed Vesicles. To determine whether or not the effect of divalent cations on vesicle adsorption is reversible, additional QCM-D experiments were performed with an adsorbed DOPC lipid vesicle layer on titanium oxide (Figure 5). In the first set of experiments, vesicles were suspended in 10 mM Tris buffer [pH 7.5] with 150 mM NaCl and 5 mM $CaCl_2$ and then deposited on the substrate, yielding Δf and ΔD shifts of approximately −140 Hz and 12×10^{-6}, respectively (Figure 5A). The solution in the measurement chamber was then exchanged to 10 mM Tris buffer [pH 7.5] with 150 mM NaCl and no $CaCl_2$, in effect removing Ca^{2+} from the system.[49] Upon this exchange, there were Δf and ΔD shifts of approximately −2 Hz and 1.2×10^{-6}, respectively. When the solution was exchanged back to the original buffer, the Δf and ΔD shifts nearly returned back to the original values and cycling was performed in order to demonstrate that the effect on the QCM-D measurement signals is reversible and there is minimal hysteresis. By contrast, exchange of the two buffer solutions (without and with 5 mM $CaCl_2$) on bare titanium oxide and silicon oxide surfaces yielded appreciably smaller Δf and ΔD shifts, indicating that the measurement response is specific to the adsorbed vesicle layer and not due to a change in the properties of the bulk solution alone (Figures S2 and S3). Moreover, on titanium oxide, introduction of the buffer solution with 5 mM $CaCl_2$ led to a negative frequency shift on the bare substrate, while the same exchange led to a positive frequency shift for the adsorbed vesicle layer case. All lines of evidence point to the observed Δf and ΔD shifts arising from changes in properties of the vesicle adlayer. As further confirmation, the opposite case of vesicle adsorption was also investigated whereby vesicles were initially deposited in 10 mM Tris buffer [pH 7.5] with 150 mM NaCl and no $CaCl_2$, and then the solution was exchanged to 10 mM Tris buffer [pH 7.5] with 150 mM NaCl and 5 mM $CaCl_2$ (Figure 5B). Again, the effect on the measurement signals was reversible and nearly identical. Voigt−Voinova model analysis[50] was also employed in order to account for the viscoelastic properties of the adsorbed vesicle layers in the presence and absence of 5 mM $CaCl_2$. Accordingly, the effective Voigt thickness of the adsorbed vesicle layer was determined to be 56 nm without Ca^{2+} and 53 nm with Ca^{2+}, lending further support to the tentative conclusion that divalent cations increase the deformation of adsorbed vesicles.

LSPR Measurements. In order to further investigate the vesicle adsorption process, LSPR experiments were performed to measure the relative extent of vesicle deformation. Changes in the LSPR peak position ($\Delta\lambda_{max}$) were monitored as a function of time. The peak position is sensitive to the local refractive index surrounding the dielectric-coated gold nanodisks so vesicle adsorption induces an increase in the peak position because the refractive index of lipid molecules is greater than the refractive index of the buffer solution. In all experiments, a baseline signal was first recorded in the appropriate buffer solution followed by the addition of 0.05 mg/mL lipid vesicles in an identical buffer solution at t = 5 min. The results obtained on the silicon oxide and titanium oxide substrates are reported below.

Silicon Oxide. Figure 6 presents the change in peak shift (centroid position of the extinction wavelength[51]) as a function of time upon vesicle addition to silicon oxide-coated gold nanodisks. Initially, a constant rate of change in the LSPR signal is observed due to diffusion-limited vesicle adsorption followed by rate acceleration after ∼6 min. This kink is attributed to vesicle rupture and the onset of SLB formation resulting in the net movement of lipids toward the sensor surface.[23] The final peak shift values were around 3 nm in all cases and the adsorption kinetics indicate SLB formation. Upon close inspection of the kinetic curves, it is apparent that the initial slope of the rate of change in the LSPR signal for the Ca^{2+} case is greater than in the other cases (Figure 6, inset). Because the diffusion flux of vesicle adsorption onto the substrate is the same in all cases, the increased rate of change in the LSPR signal is attributed to greater vesicle deformation induced by Ca^{2+} because the lipids in a more deformed vesicle are nearer, on average, to the sensor surface than in a less deformed vesicle.[15] Likewise, the next highest rate of change in the LSPR signal is in the Mg^{2+} case, followed by the Sr^{2+} and control

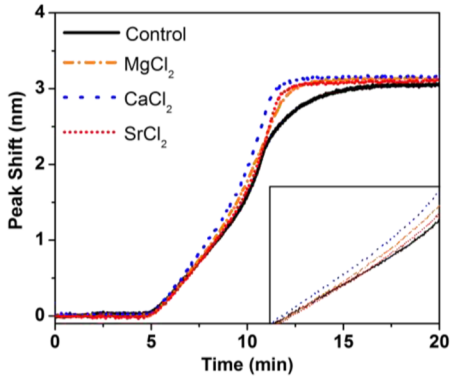

Figure 6. Influence of divalent cations on the deformation of adsorbed vesicles on silicon oxide. LSPR measurements were performed, and vesicles were added at t = 5 min. The shift in the centroid position of the extinction wavelength is reported as a function of time. The inset shows the onset of the kinetics in more detail.

DOI: 10.1021/acs.langmuir.6b00439
Langmuir 2016, 32, 6486−6495

cases. Among the divalent cations, increased deformation of adsorbed vesicles is observed in the order, $Ca^{2+} > Mg^{2+} > Sr^{2+}$, which agrees well with the QCM-D measurements on silicon oxide. As a control experiment, we determined that, after the SLB was formed, cycling between Ca^{2+}-free and Ca^{2+}-containing buffer had negligible effect on the peak shift (data not shown). In addition to the observed effect on vesicle deformation, the LSPR measurements also indicate that the presence of divalent cations accelerates the vesicle rupture process as indicated by the time scale between the kink in the LSPR signal and stabilization of the LSPR signal upon SLB formation.

Titanium Oxide. Figure 7 presents the corresponding change in peak shift as a function of time upon vesicle addition to

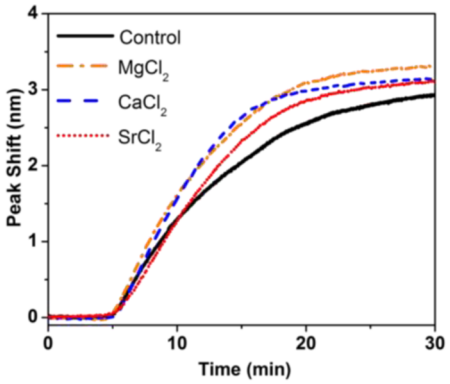

Figure 7. Influence of divalent cations on deformation of adsorbed vesicles on titanium oxide. LSPR measurements were performed and vesicles were added at t = 5 min. The shift in the centroid position of the extinction wavelength is reported as a function of time.

titanium oxide-coated gold nanodisks. In all cases, a monotonic increase was observed until reaching saturation of adsorbed vesicles. The final peak shifts were around 3 nm but there was no rate acceleration, indicating that vesicles adsorbed but did not rupture. Again, the initial rate of change in the LSPR signal provides insight into the relative extent of vesicle deformation, and the greatest slopes were observed for the Ca^{2+} and Mg^{2+} cases. An intermediate-size slope was obtained in the Sr^{2+} case, and the smallest slope was recorded for the control experiment without divalent cations. Altogether, the data are consistent with the QCM-D measurements on titanium oxide which suggested that divalent cations increase the deformation of adsorbed vesicles, with the greatest effect attributed to Ca^{2+} ions.

DISCUSSION

One of the main goals of our study was to identify the effect of various divalent ions on the deformation of adsorbed vesicles. While the QCM-D data (cf. Figures 2–5) offer strong evidence to support that divalent cations have significant effects on the deformation of adsorbed vesicles, their quantitative interpretation to directly estimate the relative extent of vesicle deformation is challenging. On the other hand, the LSPR data (cf. Figures 6 and 7) can be interpreted by using a model describing the mutual light-induced interaction of gold nanodisk sensors and deformed vesicles.[15,35] The model operates with the following parameters: the effective radius R_* characterizing the gold nanodisks; the radius of non-deformed vesicles, r; and the radius a of the vesicle-surface contact area after adsorption and deformation of vesicles, which are described as truncated spheres (Figure 8A). Geometrically,

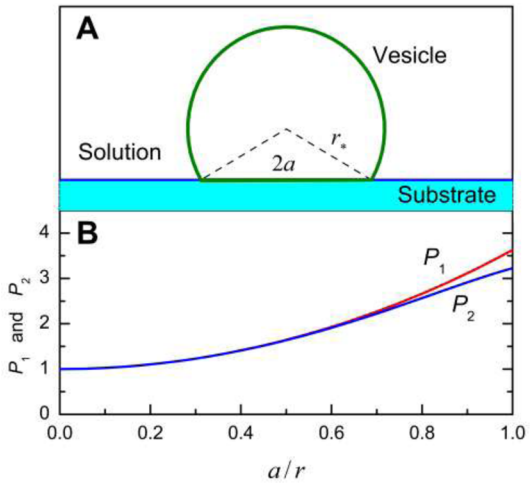

Figure 8. Characterization of the effect of deformation of adsorbed vesicles on the LSPR signal. (A) A deformed vesicle is represented as a truncated sphere. (B) Dimensionless parameters P_1 and P_2 as a function of a/r for r = 38 nm and R_* = 74 nm (according to eqs 10 and 13 from ref 15).

vesicle deformation is characterized by the dimensionless parameter $p \equiv a/r$, whereby $p = 0$ corresponds to the case of nondeformed vesicles, while $p \approx 1$ is for appreciable deformation (formally, p may be in the range from 0 up to $2^{1/2}$, but at $p > 1$ the deformation is so strong that such vesicles are expected to rupture). To characterize the deformation of vesicles in the context of the LSPR measurements, it is convenient also to introduce[15] two dimensionless parameters, P_1 and P_2. The former one, P_1, is defined as the ratio of the LSPR wavelength shifts for adsorbed vesicles in the deformed and nondeformed states, respectively, provided the vesicle surface concentration is below saturation and the same irrespective of the extent of deformation. The latter one, P_2, is a similar ratio that is calculated provided vesicles are at saturation in the close-packed state. This model was used to interpret the effect of temperature on adsorption and deformation of DOPC and DPPC lipid vesicles on titanium oxide.[15] Recently, it was validated by detailed 3D finite difference time-domain simulations.[25] In particular, the suitable value of R_* was determined to be 74 nm for the gold nanodisk sensors. Using this value in combination with r = 38 nm (this corresponds to the vesicles under consideration), we calculated P_1 and P_2 as a function of p (Figure 8B).

To apply this model, we note that the present LSPR measurements on silicon oxide indicate that the addition of divalent ions results in an increase of the LSPR shift by ≤10% compared to the reference case (e.g., at t = 10 min as shown in Figure 6). In such measurements, the LSPR wavelength shift corresponding to nondeformed vesicles cannot be determined. For this reason, to estimate theoretically the extent of the ion-related vesicle deformation, we should postulate the extent of deformation in the reference state. Assuming that this state is characterized by a/r = 0.5 and P_1 = 1.64 (cf. Figure 8B), we reason that the 10% shift in the LSPR signal corresponds to a/r = 0.56 and P_1 = 1.80. In the case of titanium oxide, the scale of the ion-related increase of the LSPR signal is 25% (e.g., at t = 15 min in Figure 7). Assuming that deformation in the

DOI: 10.1021/acs.langmuir.6b00439
Langmuir 2016, 32, 6486–6495

reference state is here negligible, i.e., $a/r = 0$ and $P_1 = 1$ (because there is no rupture), we obtain that this shift corresponds to $a/r = 0.32$ and $P_1 = 1.26$. This analysis shows that, on both surfaces, the ion-induced deformation is modest.

Turning to the question of how divalent cations promote increased deformation of adsorbed vesicles, we recall the discussion of relevant factors presented by Seantier and Kasemo,[38] including the influence of vesicle−substrate interaction, the cohesive strength of vesicles, and vesicle−vesicle interactions. The overall situation is complex and nuanced. Here, we discuss the pertinent factors in the context of our experimental findings and the earlier tentative mechanistic scenario postulated in the aforementioned study[38] that divalent cations strengthen the vesicle−substrate interaction leading to greater deformation of adsorbed vesicles. Specifically, it was suggested[38] that attachment of divalent cations to the phosphate group in PC lipid headgroups would in effect induce a positive monopole that strengthens the interaction of vesicles with negatively charged silicon oxide surfaces. At the time, the QCM-D measurements in this former study[38] pointed to Mg^{2+} ions inducing the greatest deformation of adsorbed POPC lipid vesicles among the tested divalent cations. In order to rationalize the experimental trend that Mg^{2+} had the greatest promoting effect on POPC SLB formation vis-à-vis increased vesicle deformation, it was suggested that there is "stronger binding to the PCs for Mg^{2+}" which contributed to a strong vesicle−substrate interaction.[38]

To clarify the situation and extend the tentative mechanistic model to other zwitterionic lipids, we have utilized two complementary measurement techniques in order to probe the effects of divalent cations on DOPC lipid vesicle adsorption and deformation. While POPC and DOPC are both zwitterionic lipids, they have different numbers of unsaturated tails which affect lipid packing and divalent cation adsorption onto the lipid headgroups.[46] As a result, these subtle differences can likely result in differing effects of how specific divalent cations influence vesicle adsorption, deformation, and rupture leading to SLB formation. Indeed, in the present study, the collective set of QCM-D and LSPR experiments identified that Ca^{2+} ions not only had the greatest promoting effect on DOPC SLB formation, but also promote increased DOPC lipid vesicle deformation on silicon oxide more so than Mg^{2+} and Sr^{2+} ions. This finding is consistent with the known high binding affinity of Ca^{2+} to the phosphate group of PC lipid headgroups, and several previous experimental studies[46,52−58] have indicated that Ca^{2+} ions have a higher binding affinity to PC lipids than Mg^{2+} ions. Recent molecular dynamics simulations also indicate that the interaction of a Ca^{2+} ion with the interior of PC lipid headgroups is energetically favorable (the corresponding energy gain is about 16 kcal/mol), while a Mg^{2+} ion has a strong affinity to hydration water, which makes direct binding to the lipid headgroup difficult.[59] Interestingly, our findings show that Ca^{2+} ions have the greatest promoting effect for DOPC SLB formation while the past work indicated that Mg^{2+} ions have the greatest promoting effect for POPC SLB formation. While these different results may arise from differences in physicochemical properties of the two lipids (e.g., packing state), they may also be influenced by details of the specific measurement setups, including flow configuration, vesicle size, buffer condition and substrate cleaning procedure. Importantly, regardless of these minor differences, our findings strongly support the previous study[38] and provide direct evidence that divalent cations promote increased deformation of adsorbed, zwitterionic lipid vesicles on both silicon oxide and titanium oxide, with Ca^{2+} and Mg^{2+} cations exhibiting the most prominent effects.

According to our analysis, the effect of divalent ions on vesicle deformation is modest. On the other hand, the effects of these ions on vesicle rupture on silicon oxide are modest as well. From this perspective, our results concerning vesicle deformation and rupture are consistent. With this reservation, we may finally articulate that the vesicle deformation is only one factor influencing the fate of adsorbed vesicles. In vesicle rupture on silicon oxide, as already noticed in the Introduction, the vesicle−vesicle interaction is also important, and, accordingly, the better fusogenic ability of Ca^{2+} (see, e.g., ref 60 and references therein) is another relevant factor for the explanation of our results, especially in the moderate and high surface coverage regime. Taken together, the QCM-D and LSPR experimental results offer conclusive evidence that divalent cations increase the deformation of adsorbed vesicles on silicon oxide and titanium oxide.

CONCLUSION

In summary, the findings presented in this work clarify the role of divalent cations in modulating vesicle−substrate interaction, further strengthening our growing knowledge of the SLB formation process through the vesicle fusion method while shedding light on the nuanced effects of ions on lipid membranes. The work also highlights the potential of employing the complementary QCM-D and LSPR measurement techniques in order to unravel details of vesicle adsorption and deformation at solid surfaces as well as other related soft matter phenomena.

ASSOCIATED CONTENT

Supporting Information

The Supporting Information is available free of charge on the ACS Publications website at DOI: 10.1021/acs.langmuir.6b00439.

More detailed information is provided about the effects of divalent cations on the kinetics of vesicle adsorption and rupture (Figure S1) as well as control experiments on bare silicon oxide and titanium oxide substrates (Figures S2 and S3) (PDF)

AUTHOR INFORMATION

Corresponding Author

*E-mail: njcho@ntu.edu.sg.

Author Contributions

#These authors contributed equally to this work.

Notes

The authors declare no competing financial interest.

ACKNOWLEDGMENTS

The authors acknowledge support from the National Research Foundation (NRF-NRFF2011-01). V.P.Zh. is a recipient of the Tan Chin Tuan Exchange Fellowship at Nanyang Technological University. M.D. was supported by the Pomona College Summer Research Experience Scholarship.

REFERENCES

(1) van Meer, G.; Voelker, D. R.; Feigenson, G. W. Membrane lipids: where they are and how they behave. *Nat. Rev. Mol. Cell Biol.* **2008**, *9* (2), 112−124.

DOI: 10.1021/acs.langmuir.6b00439
Langmuir 2016, 32, 6486−6495

(2) Lingwood, D.; Simons, K. Lipid rafts as a membrane-organizing principle. *Science* **2010**, *327* (5961), 46−50.
(3) Richter, R. P.; Bérat, R.; Brisson, A. R. Formation of Solid-Supported Lipid Bilayers: An Integrated View. *Langmuir* **2006**, *22* (8), 3497−3505.
(4) Chan, Y.-H. M.; Boxer, S. G. Model membrane systems and their applications. *Curr. Opin. Chem. Biol.* **2007**, *11* (6), 581−587.
(5) Hardy, G. J.; Nayak, R.; Zauscher, S. Model cell membranes: Techniques to form complex biomimetic supported lipid bilayers via vesicle fusion. *Curr. Opin. Colloid Interface Sci.* **2013**, *18* (5), 448−458.
(6) Castellana, E. T.; Cremer, P. S. Solid supported lipid bilayers: From biophysical studies to sensor design. *Surf. Sci. Rep.* **2006**, *61* (10), 429−444.
(7) Höök, F.; Stengel, G.; Dahlin, A. B.; Gunnarsson, A.; Jonsson, M. P.; Jönsson, P.; Reimhult, E.; Simonsson, L.; Svedhem, S. Supported lipid bilayers, tethered lipid vesicles, and vesicle fusion investigated using gravimetric, plasmonic, and microscopy techniques. *Biointerphases* **2008**, *3* (2), FA108−FA116.
(8) Mashaghi, A.; Mashaghi, S.; Reviakine, I.; Heeren, R. M.; Sandoghdar, V.; Bonn, M. Label-free characterization of biomembranes: from structure to dynamics. *Chem. Soc. Rev.* **2014**, *43* (3), 887−900.
(9) Keller, C. A.; Kasemo, B. Surface specific kinetics of lipid vesicle adsorption measured with a quartz crystal microbalance. *Biophys. J.* **1998**, *75* (3), 1397−1402.
(10) Reimhult, E.; Höök, F.; Kasemo, B. Intact Vesicle Adsorption and Supported Biomembrane Formation from Vesicles in Solution: Influence of Surface Chemistry, Vesicle Size, Temperature, and Osmotic Pressure†. *Langmuir* **2003**, *19* (5), 1681−1691.
(11) Richter, R.; Mukhopadhyay, A.; Brisson, A. Pathways of lipid vesicle deposition on solid surfaces: a combined QCM-D and AFM study. *Biophys. J.* **2003**, *85* (5), 3035−3047.
(12) Rossetti, F. F.; Bally, M.; Michel, R.; Textor, M.; Reviakine, I. Interactions between Titanium Dioxide and Phosphatidyl Serine-Containing Liposomes: Formation and Patterning of Supported Phospholipid Bilayers on the Surface of a Medically Relevant Material. *Langmuir* **2005**, *21* (14), 6443−6450.
(13) Gulcev, M. D.; Lucy, C. A. Factors affecting the behavior and effectiveness of phospholipid bilayer coatings for capillary electrophoretic separations of basic proteins. *Anal. Chem.* **2008**, *80* (5), 1806−1812.
(14) Cremer, P. S.; Boxer, S. G. Formation and spreading of lipid bilayers on planar glass supports. *J. Phys. Chem. B* **1999**, *103* (13), 2554−2559.
(15) Oh, E.; Jackman, J. A.; Yorulmaz, S.; Zhdanov, V. P.; Lee, H.; Cho, N.-J. Contribution of Temperature to Deformation of Adsorbed Vesicles Studied by Nanoplasmonic Biosensing. *Langmuir* **2015**, *31* (2), 771−781.
(16) Boudard, S.; Seantier, B.; Breffa, C.; Decher, G.; Felix, O. Controlling the pathway of formation of supported lipid bilayers of DMPC by varying the sodium chloride concentration. *Thin Solid Films* **2006**, *495* (1), 246−251.
(17) Tero, R. Substrate effects on the formation process, structure and physicochemical properties of supported lipid bilayers. *Materials* **2012**, *5* (12), 2658−2680.
(18) Raedler, J.; Strey, H.; Sackmann, E. Phenomenology and Kinetics of Lipid Bilayer Spreading on Hydrophilic Surfaces. *Langmuir* **1995**, *11* (11), 4539−4548.
(19) Reviakine, I.; Rossetti, F. F.; Morozov, A. N.; Textor, M. Investigating the properties of supported vesicular layers on titanium dioxide by quartz crystal microbalance with dissipation measurements. *J. Chem. Phys.* **2005**, *122* (20), 204711.
(20) Tawa, K.; Morigaki, K. Substrate-Supported Phospholipid Membranes Studied by Surface Plasmon Resonance and Surface Plasmon Fluorescence Spectroscopy. *Biophys. J.* **2005**, *89* (4), 2750−2758.
(21) Reviakine, I.; Brisson, A. Formation of supported phospholipid bilayers from unilamellar vesicles investigated by atomic force microscopy. *Langmuir* **2000**, *16* (4), 1806−1815.
(22) Andrecka, J.; Spillane, K. M.; Ortega-Arroyo, J.; Kukura, P. Direct Observation and Control of Supported Lipid Bilayer Formation with Interferometric Scattering Microscopy. *ACS Nano* **2013**, *7* (12), 10662−10670.
(23) Jonsson, M. P.; Jönsson, P.; Dahlin, A. B.; Höök, F. Supported lipid bilayer formation and lipid-membrane-mediated biorecognition reactions studied with a new nanoplasmonic sensor template. *Nano Lett.* **2007**, *7* (11), 3462−3468.
(24) Tero, R.; Ujihara, T.; Urisu, T. Lipid bilayer membrane with atomic step structure: supported bilayer on a step-and-terrace TiO2 (100) surface. *Langmuir* **2008**, *24* (20), 11567−11576.
(25) Jackman, J. A.; Spackova, B.; Linardy, E.; Kim, M. C.; Yoon, B. K.; Homola, J.; Cho, N.-J. Nanoplasmonic ruler to measure lipid vesicle deformation. *Chem. Commun.* **2016**, *52* (1), 76−79.
(26) Hamai, C.; Yang, T.; Kataoka, S.; Cremer, P. S.; Musser, S. M. Effect of average phospholipid curvature on supported bilayer formation on glass by vesicle fusion. *Biophys. J.* **2006**, *90* (4), 1241−1248.
(27) Hamai, C.; Cremer, P. S.; Musser, S. M. Single giant vesicle rupture events reveal multiple mechanisms of glass-supported bilayer formation. *Biophys. J.* **2007**, *92* (6), 1988−1999.
(28) Dimitrievski, K. Deformation of adsorbed lipid vesicles as a function of vesicle size. *Langmuir* **2010**, *26* (5), 3008−3011.
(29) Zhdanov, V.; Kasemo, B. Comments on rupture of adsorbed vesicles. *Langmuir* **2001**, *17* (12), 3518−3521.
(30) Dimitrievski, K.; Kasemo, B. Simulations of Lipid Vesicle Adsorption for Different Lipid Mixtures. *Langmuir* **2008**, *24* (8), 4077−4091.
(31) Hain, N.; Gallego, M.; Reviakine, I. Unraveling Supported Lipid Bilayer Formation Kinetics: Osmotic Effects. *Langmuir* **2013**, *29* (7), 2282−2288.
(32) Zhu, T.; Jiang, Z.; Nurlybaeva, E. M. R.; Sheng, J.; Ma, Y. Effect of Osmotic Stress on Membrane Fusion on Solid Substrate. *Langmuir* **2013**, *29* (21), 6377−6385.
(33) Zhdanov, V. P. Mechanism of rupture of single adsorbed vesicles. *Chem. Phys. Lett.* **2015**, *641*, 20−22.
(34) Schönherr, H.; Johnson, J. M.; Lenz, P.; Frank, C. W.; Boxer, S. G. Vesicle adsorption and lipid bilayer formation on glass studied by atomic force microscopy. *Langmuir* **2004**, *20* (26), 11600−11606.
(35) Jackman, J. A.; Zhdanov, V. P.; Cho, N.-J. Nanoplasmonic Biosensing for Soft Matter Adsorption: Kinetics of Lipid Vesicle Attachment and Shape Deformation. *Langmuir* **2014**, *30* (31), 9494−9503.
(36) Garcia-Manyes, S.; Oncins, G.; Sanz, F. Effect of Ion-Binding and Chemical Phospholipid Structure on the Nanomechanics of Lipid Bilayers Studied by Force Spectroscopy. *Biophys. J.* **2005**, *89* (3), 1812−1826.
(37) Ekeroth, J.; Konradsson, P.; Höök, F. Bivalent-ion-mediated vesicle adsorption and controlled supported phospholipid bilayer formation on molecular phosphate and sulfate layers on gold. *Langmuir* **2002**, *18* (21), 7923−7929.
(38) Seantier, B.; Kasemo, B. Influence of Mono- And Divalent Ions on the Formation of Supported Phospholipid Bilayers via Vesicle Adsorption. *Langmuir* **2009**, *25* (10), 5767−5772.
(39) Dahlin, A.; Zäch, M.; Rindzevicius, T.; Käll, M.; Sutherland, D. S.; Höök, F. Localized surface plasmon resonance sensing of lipid-membrane-mediated biorecognition events. *J. Am. Chem. Soc.* **2005**, *127* (14), 5043−5048.
(40) Beneš, M.; Billy, D.; Benda, A.; Speijer, H.; Hof, M.; Hermens, W. T. Surface-dependent transitions during self-assembly of phospholipid membranes on mica, silica, and glass. *Langmuir* **2004**, *20* (23), 10129−10137.
(41) Berquand, A.; Lévy, D.; Gubellini, F.; Le Grimellec, C.; Milhiet, P.-E. Influence of calcium on direct incorporation of membrane proteins into in-plane lipid bilayer. *Ultramicroscopy* **2007**, *107* (10−11), 928−933.
(42) Zhu, T.; Xu, F.; Yuan, B.; Ren, C.; Jiang, Z.; Ma, Y. Effect of calcium cation on lipid vesicle deposition on silicon dioxide surface under various thermal conditions. *Colloids Surf., B* **2012**, *89*, 228−233.

DOI: 10.1021/acs.langmuir.6b00439
Langmuir 2016, 32, 6486−6495

(43) Seantier, B.; Breffa, C.; Félix, O.; Decher, G. Dissipation-Enhanced Quartz Crystal Microbalance Studies on the Experimental Parameters Controlling the Formation of Supported Lipid Bilayers. *J. Phys. Chem. B* **2005**, *109* (46), 21755−21765.
(44) Oleson, T. A.; Sahai, N. Oxide-dependent adsorption of a model membrane phospholipid, dipalmitoylphosphatidylcholine: bulk adsorption isotherms. *Langmuir* **2008**, *24* (9), 4865−4873.
(45) Oleson, T. A.; Sahai, N.; Pedersen, J. A. Electrostatic effects on deposition of multiple phospholipid bilayers at oxide surfaces. *J. Colloid Interface Sci.* **2010**, *352* (2), 327−336.
(46) Szekely, O.; Steiner, A.; Szekely, P.; Amit, E.; Asor, R.; Tamburu, C.; Raviv, U. The structure of ions and zwitterionic lipids regulates the charge of dipolar membranes. *Langmuir* **2011**, *27* (12), 7419−7438.
(47) MacDonald, R. C.; MacDonald, R. I.; Menco, B. P. M.; Takeshita, K.; Subbarao, N. K.; Hu, L.-r. Small-volume extrusion apparatus for preparation of large, unilamellar vesicles. *Biochim. Biophys. Acta, Biomembr.* **1991**, *1061* (2), 297−303.
(48) Keller, C.; Glasmästar, K.; Zhdanov, V.; Kasemo, B. Formation of supported membranes from vesicles. *Phys. Rev. Lett.* **2000**, *84* (23), 5443−5446.
(49) Kunze, A.; Zhao, F.; Marel, A.-K.; Svedhem, S.; Kasemo, B. Ion-mediated changes of supported lipid bilayers and their coupling to the substrate. A case of bilayer slip? *Soft Matter* **2011**, *7* (18), 8582−8591.
(50) Voinova, M.; Jonson, M.; Kasemo, B. 'Missing mass' effect in biosensor's QCM applications. *Biosens. Bioelectron.* **2002**, *17* (10), 835−841.
(51) Dahlin, A. B.; Tegenfeldt, J. O.; Höök, F. Improving the instrumental resolution of sensors based on localized surface plasmon resonance. *Anal. Chem.* **2006**, *78* (13), 4416−4423.
(52) Lis, L.; Rand, R.; Parsegian, V., Measurement of the Adsorption of Ca^{2+} and Mg^{2+} to Phosphatidyl Choline Bilayers. In 1980.
(53) Lau, A. L.; McLaughlin, A. C.; MacDonald, R. C.; McLaughlin, S. G. The adsorption of alkaline earth cations to phosphatidyl choline bilayer membranes: a unique effect of calcium. *Adv. Chem. Ser.* **1980**, *188*, 49−56.
(54) Lis, L.; Lis, W.; Parsegian, V.; Rand, R. Adsorption of divalent cations to a variety of phosphatidylcholine bilayers. *Biochemistry* **1981**, *20* (7), 1771−1777.
(55) Lis, L.; Parsegian, V.; Rand, R. Binding of divalent cations to dipalmitoylphosphatidylcholine bilayers and its effect on bilayer interaction. *Biochemistry* **1981**, *20* (7), 1761−1770.
(56) Kataoka, R.; Aruga, S.; Mitaku, S.; Kinosita, K.; Ikegami, A. Interaction between Ca^{2+} and dipalmitoylphosphatidylcholine membranes: II. Fluorescence anisotropy study. *Biophys. Chem.* **1985**, *21* (3), 277−284.
(57) Marra, J.; Israelachvili, J. Direct measurements of forces between phosphatidylcholine and phosphatidylethanolamine bilayers in aqueous electrolyte solutions. *Biochemistry* **1985**, *24* (17), 4608−4618.
(58) Zidovetzki, R.; Atiya, A. W.; Boeck, H. D. Effect of divalent cations on the structure of dipalmitoylphosphatidylcholine and phosphatidylcholine/phosphatidylglycerol bilayers: an 2H-NMR study. *Membr. Biochem.* **1989**, *8* (3), 177−186.
(59) Yang, J.; Calero, C.; Bonomi, M.; Martí, J. Specific Ion Binding at Phospholipid Membrane Surfaces. *J. Chem. Theory Comput.* **2015**, *11* (9), 4495−4499.
(60) Issa, Z. K.; Manke, C. W.; Jena, B. P.; Potoff, J. J. Ca^{2+} bridging of apposed phospholipid bilayers. *J. Phys. Chem. B* **2010**, *114* (41), 13249−13254.

DOI: 10.1021/acs.langmuir.6b00439
Langmuir 2016, 32, 6486−6495